

Decipher the dynamic coordination between enzymatic activity and structural modulation at focal adhesions in living cells

Shaoying Lu^{1,2}, Jihye Seong^{3,6}, Yi Wang², Shiou-chi Chang⁴, John Paul Eichorst⁵, Mingxing Ouyang^{1,2}, Julie Y.-S. Li¹, Shu Chien^{1*}, Yingxiao Wang^{1,2,3,5*}

¹Department of Bioengineering, Institute of Engineering in Medicine, University of California, San Diego, La Jolla, CA 92093-0435; ²Department of Bioengineering, ³Neuroscience Program, ⁴Department of Chemical Engineering, ⁵Center of Biophysics and Computational Biology, Beckman Institute for Advanced Science and Technology, Department of Molecular and Integrative Physiology and, University of Illinois at Urbana-Champaign, Urbana, IL 61801; ⁶Currently at Korea Institute of Science and Technology (KIST), Seoul, South Korea.

SUPPLEMENTARY METHODS

Here we provide detailed description of CFIM, including the modification of the water algorithm, the customized cross-correlation function, and a discussion about the dependency between the correlation coefficient and the slope in the linear regression analysis.

The modification of the water algorithm

As in the original water algorithm, fluorescent images were high-pass filtered with the window size of 61x61 pixels which was equivalent to $9.5 \times 9.5 \mu\text{m}^2$, to remove background fluorescence near nucleus^{1,2}. The size of filter was chosen to be bigger than the estimated size of FAs but less than that of the cells for optimal results. The images were then normalized by the total paxillin intensity from the whole cell before the segmentation and detection of the FA masks. An FA mask image hence has values 1 at pixels located inside of FA and 0 outside. In the water algorithm, the filtered image was segmented with a sequence of thresholds to differentiate neighboring FA sites connected to each other. This method has been widely used to detect FA sites with high accuracy^{1,3}. However, the computation speed of this method was hampered by the need of adaptive image segmentation with multiple thresholds and to merge these results. This problem can pose a serious issue for the quantification of dynamics of cellular signals because a large number of video images need to be processed. Therefore, we replaced the multiple segmentation steps by a single image segmentation step to improve the computation speed without affecting the accuracy of FA detection.

The cross-correlation between Src activation and Lam-FA disassembly

The discrete cross-correlation function (CC) between the signals A and B (A-B CC curve) were defined in the methods section

$$CC(A, B, k) = \frac{\sum_{i=1}^n A(i)B(i+k)}{\left(\sum_{i=1}^n A(i)^2\right)^{1/2} \left(\sum_{i=1}^n B(i)^2\right)^{1/2}}$$

where,

$$k = \{-m, -(m-1), \dots, -3, -2, -1, 0, 1, 2, 3, \dots, m-1, m\}, \quad m < n; \quad A = \{A(1), A(2), \dots, A(n)\}, \quad \text{and} \\ B = \{B(-(m-1)), B(-(m-2)), \dots, B(0), B(1), B(2), \dots, B(n), B(n+1), \dots, B(n+k)\}.$$

In our experiments, the actual signal B_e representing the FA disassembly has the same number of data points as the signal A (*Src* activation): $B_e = \{B_e(1), B_e(2), \dots, B_e(n)\}$. Therefore, B_e needs to be extended on both sides to match the dimension of the signal B. Since the B_e signals are relatively stable both before (to the left side of B_e) and after (to the right side of B_e) PDGF stimulation (Fig. 3a), it is appropriate to extend the signals at both sides using the end values, i.e. using $B_e(1)$ toward left and $B_e(n)$ toward right. In our customized cross-correlation function, the signal B was extended by

$$B_e(-(m-1)) = B_e(-(m-2)) = \dots = B_e(0) = B_e(1), \quad \text{and} \\ B_e(n) = B_e(n+1) = \dots = B_e(n+k).$$

This customized cross-correlation function was used instead of the MATLAB functions *xcorr* or *xcov*, which inaccurately extends the B_e signals to both sides using the value zero.

SUPPLEMENTARY REFERENCES

- 1 Zamir, E. *et al.* Molecular diversity of cell-matrix adhesions. *J Cell Sci* **112 (Pt 11)**, 1655-1669 (1999).
- 2 Chan, K. T., Bennin, D. A. & Huttenlocher, A. Regulation of adhesion dynamics by calpain-mediated proteolysis of focal adhesion kinase (FAK). *J Biol Chem* **285**, 11418-11426.
- 3 Balaban, N. Q. *et al.* Force and focal adhesion assembly: a close relationship studied using elastic micropatterned substrates. *Nat Cell Biol* **3**, 466-472 (2001).

SUPPLEMENTARY FIGURE LEGENDS

Supplementary Figure 1. The FA detection and quantification methods. (a) The modified algorithm (segment) used the same CPU time (1.6 sec) as the original algorithm (water) for computing the high pass filter. However, the segment algorithm only required 0.22 sec to detect the location of the FAs in one image, 338 fold faster than the original water algorithm (74.3 sec). (b) The pseudo-colored paxillin intensity image overlaid with the cell edge (white) and the boundary of the detected FAs (black) using the water algorithm (top left and zoomed in at top right) or the modified algorithm (bottom left and zoomed in at bottom right). Both algorithms selected the same pixels for the FAs and produce the same results, although the segmentation algorithm may occasionally merge two neighboring FAs (pink arrows). (c) The pseudo-colored paxillin intensity image of a cell overlaid with the automatically detected cell edge (solid white), the dividing line between the outer layer and the rest of the cell mask (dotted white), and the boundary of FAs (solid black). Part of the cell body was outside of the image, so a fan-shaped region was outlined in dotted red and indicated by the dotted red arrow direction. The region of interest lies in between the dotted and solid white lines and within the fan region outlined by the dotted red lines. (d) The time courses of the averaged Src ECFP/FRET ratio (solid red) and the normalized total paxillin intensity (dotted blue) of FAs within the ROI shown in panel (c). Scale bars: 10 μm .

Supplementary Figure 2. The detection of Lam-FA disassembly and Src activation maxima. (a) The original (blue cross) and smoothed (solid blue line) time courses of Lam-FA (left panel) or Src activation (right panel), with the maxima of the curves detected and shown as red stars. (b) The maximal Lam-FA disassembly in the group of cells with high Src activation is significantly stronger than those with low Src activation (* p-value = 8.2e-5). (c) The correlation

between the final normalized paxillin intensity and the final normalized Src FRET ratio (averaged at 20-40 min). Each dot represents the data from an individual cell. The red line was fitted to data by linear regression. **(d)** The histogram showing the distribution of the normalized Src FRET ratio (left) and the normalized paxillin intensity (right) in (c). **(e)** The correlation between the paxillin intensity and Src FRET ratio at the end of the time courses (averaged at 20-40 min). The red line was fitted to data by linear regression. **(f)** The histogram showing the distribution of the Src FRET ratio (left) and the paxillin intensity (right) in (e).

Supplementary Figure 3. PDGF induced paxillin disassembly in SYFs stably re-substituted with Src-WT, but not those with Src-KD. **(a)** The time courses of normalized total paxillin intensity (light blue circles) for different individual MEFs and their average curve (solid blue) without the co-expression of Src FRET biosensor. **(b-c)** The time courses of normalized Src ECFP/FRET ratio (pink circles) and total paxillin intensity (light blue circles) from different individual cells, and the average curves of Src ECFP/FRET ratio (red solid line) and paxillin intensity (blue solid line) for **(b)** the SYF cells re-substituted with wild type Src (Src WT) and **(c)** the SYF cells re-substituted with kinase dead Src (Src KD). **(d)** The time courses of normalized Src ECFP/FRET ratio (pink circles) and total vinculin intensity (light blue circles) for different individual MEF cells, with the average curve of Src ECFP/FRET ratio in red solid line and vinculin intensity in blue solid line.

Supplementary Figure 4. The time courses of normalized Src activation color-coded by degree of Lam-FA disassembly in the same MEFs. The time courses are shown for the MEFs seeded on glass coated with FN: **(a)** [FN] - 10 $\mu\text{g/ml}$; **(b)** [FN] - 20 $\mu\text{g/ml}$.

Supplementary Figure 5. The blocking different integrin receptors did not significantly affect the focal adhesions before stimulation. The gray-scale basal level mCherry-paxillin

images of representative MEFs pretreated with the integrin $\alpha_5\beta_1$ antibody MAB2514 (left) and the integrin $\alpha_v\beta_3$ antibody LM609 (right).

Supplementary Figure 6. The integrin $\alpha_5\beta_1$ antibody MAB16 enhanced the Src-FA coordination in magnitude and kinetics in MEFs. The cells were seeded on 10 $\mu\text{g/ml}$ [FN] and pre-treated with MAB16 for 2 hours. **(a)** The time courses of normalized Src ECFP/FRET ratio (pink circles), its average curve (red solid line), the normalized total paxillin intensity (light blue circles) and its average curve (blue solid line) from different individual cells. **(b)** The time courses of Src activation color-coded by degree of Lam-FA disassembly in the same cells. **(c)** The max-max plot of maximal Lam-FA disassembly against maximal Src ECFP/FRET ratio change. Each dot represents the data from an individual cell. **(d)** The Src-FA CC curves (light blue circles) from different individual cells overlaid with the average CC curve (solid blue) and its \pm standard error (SEM, dashed blue lines). The average CC curve has a peak value of 0.84 with 0.5 min time delay between Src activation and Lam-FA disassembly.

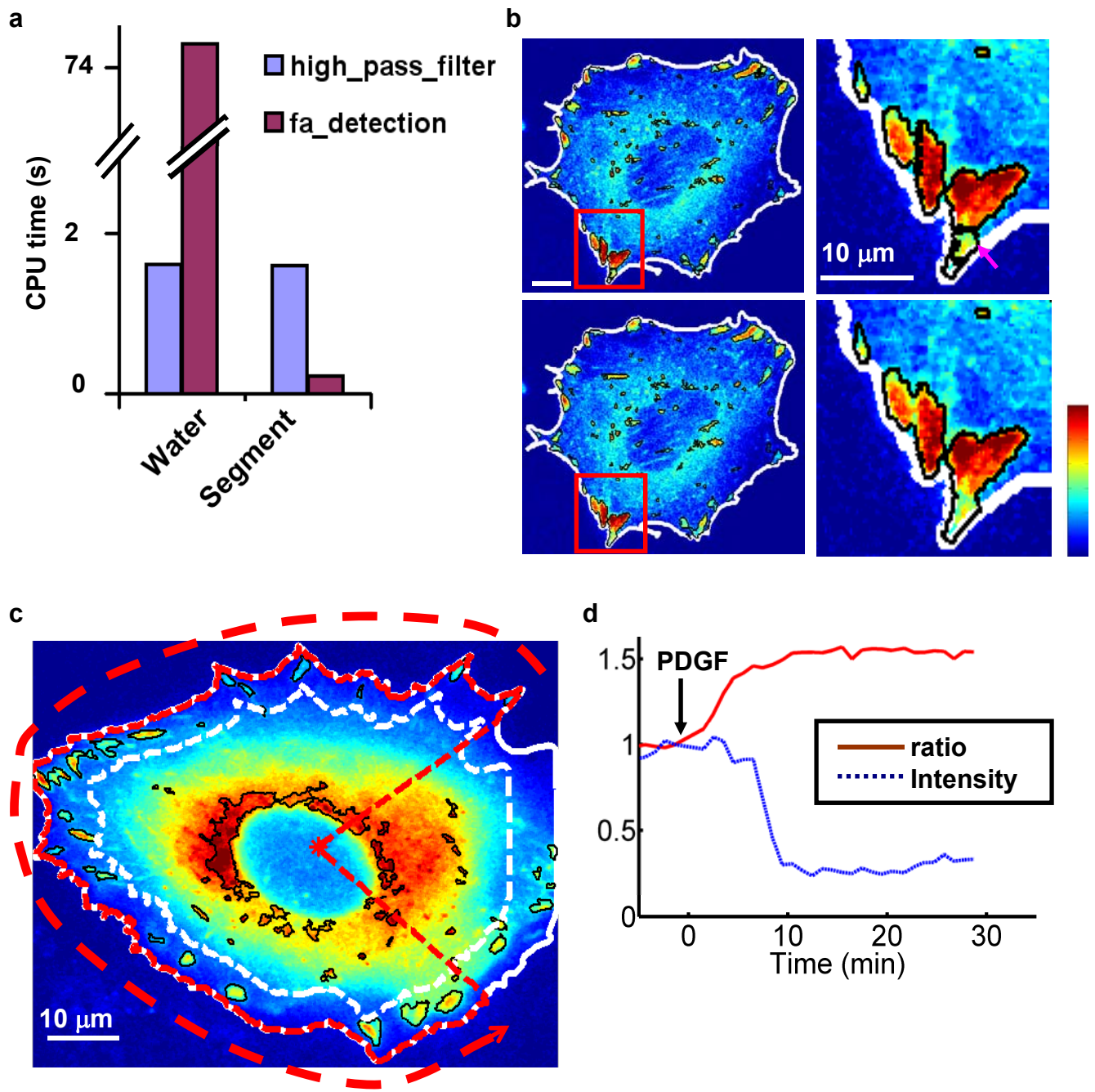
SUPPLEMENTARY VIDEO LEGENDS

Supplementary Video 1. PDGF induced Src activation and FA disassembly. Left: the Src kinase activity visualized by Src ECFP/FRET ratio; right: the paxillin-mCherry intensity representing the amount of paxillin localized in FA sites. The Src ECFP/FRET ratio turned from blue to red, and the mCherry intensity significantly decreased after PDGF stimulation.

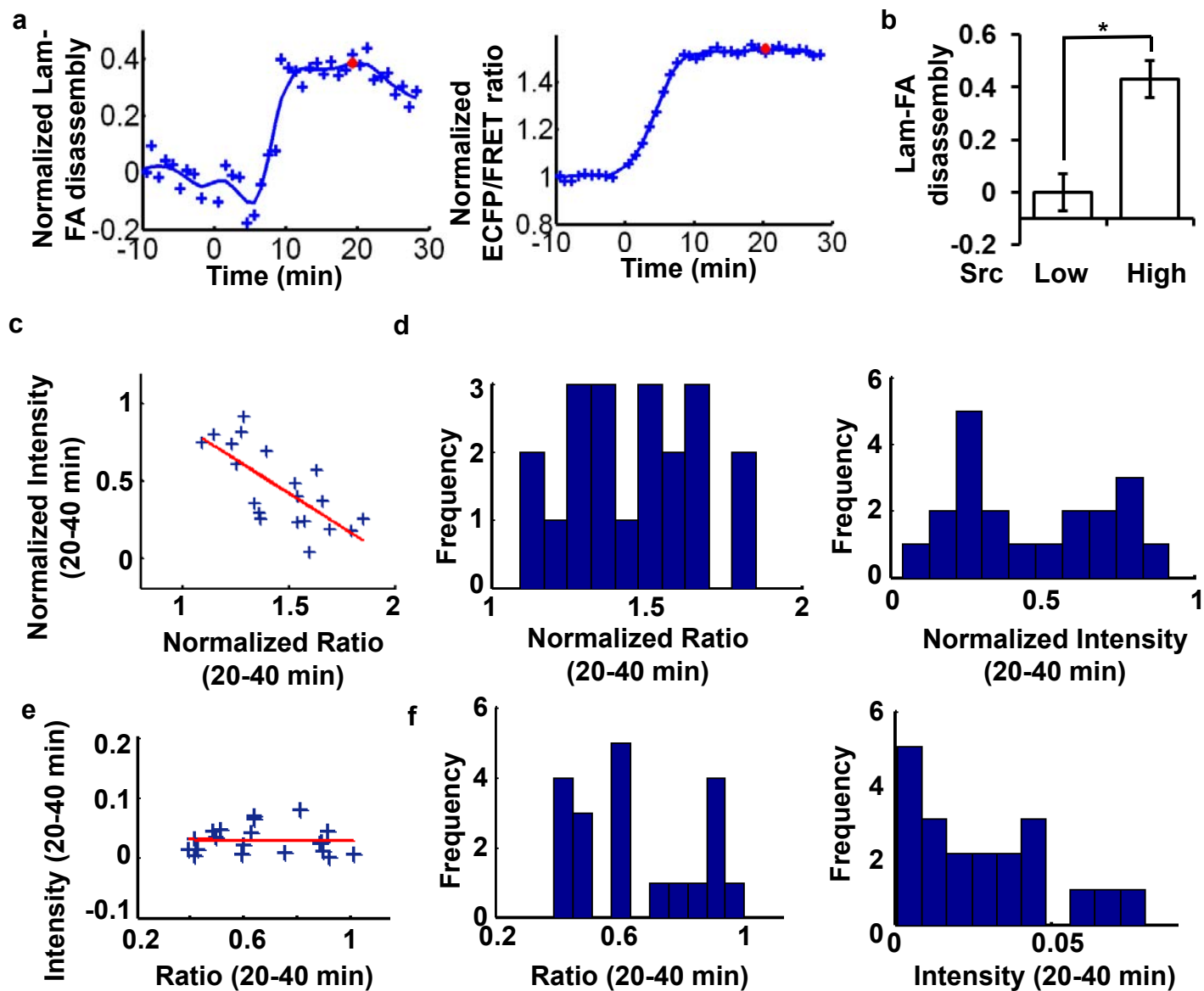
Supplementary Video 2. The automatic detection of the cell edge and the FAs. The pseudo color video image of paxillin-mCherry overlaid with detected cell edge (green), the dividing line between lamellipodia and the rest of the cell body (dashed white), and the detected FA edge outlined in black.

Supplementary Video 3. The integrin $\alpha_5\beta_1$ antibody (MAB2514) decreased the time delay between Src activation and FA disassembly. Left: the Src kinase activity visualized by Src ECFP/FRET ratio; right: the paxillin-mCherry intensity representing the amount of paxillin localized at FA sites. The Src ECFP/FRET ratio turned from blue to green simultaneously when the mCherry intensity decreased after PDGF.

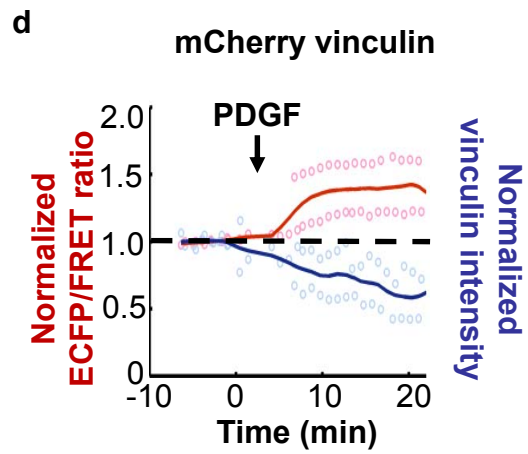
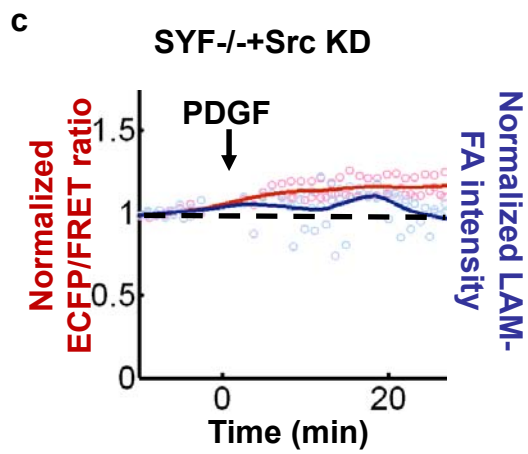
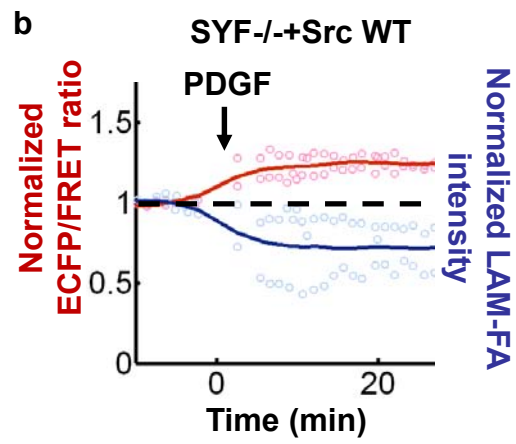
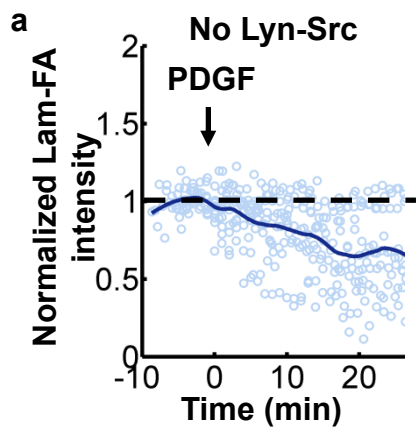
Supplementary Video 4. The integrin $\alpha_v\beta_3$ antibody (LM609) did not affect the time delay between Src activation and FA disassembly. Left: the Src kinase activity visualized by Src ECFP/FRET ratio; right: the paxillin-mCherry intensity representing the amount of paxillin localized at FA sites. The Src ECFP/FRET ratio turned from blue to red before the mCherry intensity started to decrease after PDGF.

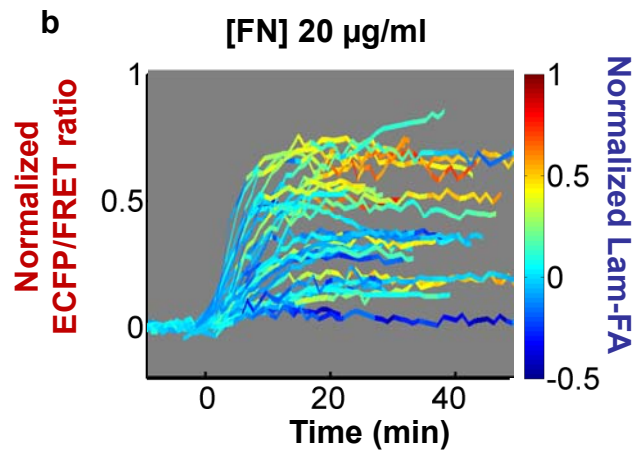
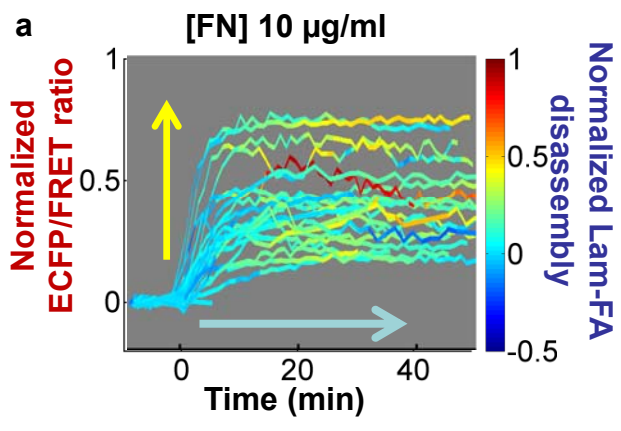


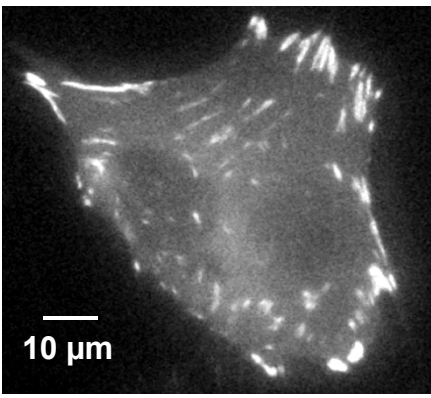
Supplementary Figure 1



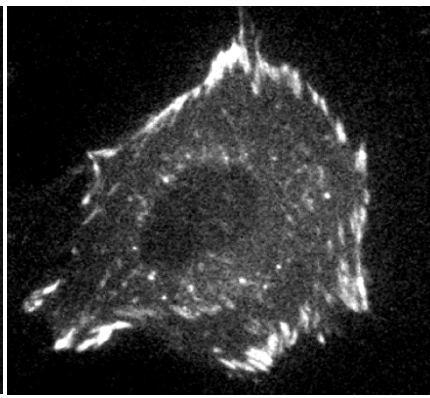
Supplementary Figure 2







– integrin $\alpha 5\beta 1$



– integrin $\alpha v\beta 3$

